Flow Field in a Tunnel with One Closed End Induced by Environmental Wind

Kaiwen Ling*, Lu Chen, Miaocheng Weng, Fang Liu, Chaopeng Sun

Chongqing university, Chongqing, China

*20165161@cqu.edu.cn

Abstract. A new closed tunnel was constructed in a real project, and most of the current studies on flow field have focused on the conventional two-opening tunnel. This study represents a pioneering investigation into the influence of ambient wind on the flow characteristics within a one-end blocked tunnel. Numerical analyses were systematically conducted encompassing diverse ambient wind speeds and directions. The findings distinctly reveal the compartmentalization of the internal flow pattern into a vortex zone and a stable zone. Moreover, the vortex zone's length displays a linear relationship with ambient wind speed and wind direction angle within a specific range. Through an amalgamation of theoretical scrutiny and empirical validation, a predictive model for the dimensionless vortex length is formulated, grounding its formulation on ambient wind speed and wind direction angle.

Keywords: Flow field, Closed end, Environmental wind.

1 Introduction

In the field of practical engineering, the blocking of tunnel exits with restrictions is a common scenario.

Scholars have extensively studied the influence of external ambient wind on the airflow within conventional tunnels through various experimental and numerical approaches. Nyman and Sanberg et al. conducted small-scale experiments to explore the effect of ambient wind on tunnel airflow [1]. Grzegorz et al. constructed wind tunnel experiments to investigate the impact of ambient wind from different directions on airflow and pressure coefficient distribution [2]. Kubwimana et al. explored the pressure difference generated by ambient wind at the tunnel entrance and established a strong correlation between pressure coefficients and tunnel aspect ratios [3]. Yao et al. performed numerical simulations to examine the relationship between flow velocity, pressure distribution, and the width-to-height ratio of the tunnel. Furthermore, Tao et al. conducted additional numerical simulations to investigate the relationship between flow velocity, pressure distribution, ambient wind, tunnel shape, and hydraulic diameter [4].In addition to the studies on airflow, several scholars have delved into the diffusion of pollutants in tunnels under the influence of ambient wind. Chow et al. developed

D. Li et al. (eds.), *Proceedings of the 2023 9th International Conference on Architectural, Civil and Hydraulic Engineering (ICACHE 2023)*, Advances in Engineering Research 228,
https://doi.org/10.2991/978-94-6463-336-8_27

a numerical simulation model to study the diffusion of carbon monoxide within tunnels exposed to ambient wind [3]. Yu Hongbin et al. conducted experiments to investigate pollutant diffusion in the tail flow at the exit of the air shaft tower of a cross river tunnel. Yang Yurong et al. performed tests on pollutants near the exit of the Beibei Tunnel and explored the influence of tunnel ventilation and smoke control system operating conditions on pollutant distribution. Additionally, Yang Yurong et al. studied the diffusion of exhaust gases at the tunnel exit under the influence of various factors through numerical simulations[5] [6]. Peng Kangfu used Fluent numerical simulations to investigate the effects of tunnel wind speed, temperature, and ambient wind on pollutant dispersion in a two-lane tunnel[7]. Chen et al. performed simulations of the flow field in an open tunnel with entrances exposed to canyon winds using Fluent simulation software[8].

Notably, existing studies exploring the impact of ambient wind on flow fields inside tunnels have solely focused on conventional tunnels. Little research has been conducted regarding the flow fields inside one-end blocked tunnels. Thus, there is a significant knowledge gap in this area that warrants further investigation in the context of one-end blocked tunnel conditions.

2 Numerical model

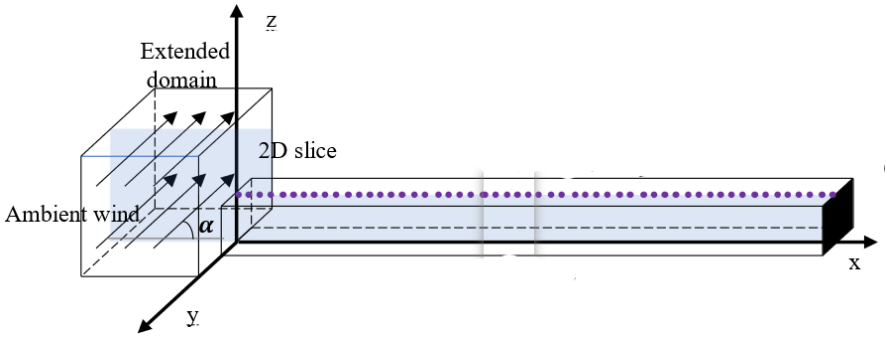

Fig. 1. FDS model of tunnel

With the development of computational fluid dynamics (CFD) and the advent of increasing computer power, it has already been possible to utilize CFD technology to analyze problems involved in three-dimensional flows in buildings[10] [11] [12].
Liang and Weng, et al., investigated the influence of wind on the flow field in a standard tunnel using FDS simulation software, demonstrating the efficacy of FDS in simulating tunnel flow dynamics [13].

The present study introduces a numerical model of a one-end blocked tunnel, illustrated in Fig. 1. The tunnel dimensions are as follows: length of 110 m, width of 10 m, and height of 5 m. A coordinate system is established with the center of the open end's bottom as the origin. The x-axis positive direction aligns with the central axis of the tunnel towards the blocked end, while the z-axis positive direction points vertically upward. All subsequent analyses in this paper are conducted based on this coordinate system. To simulate the ambient wind, an extension domain measuring 10 m × 20 m ×

10 m is established at the open end of the tunnel. A wind speed inlet boundary is defined within the extension domain for the simulation. As observed by Jing et al., the wind speed of the ambient wind outside the tunnel remains relatively stable over a considerable period, validating the use of a steady wind speed to simulate the actual conditions outside the tunnel for the sake of simulation setup convenience.

Twenty-seven sets of simulation scenarios were designed for ambient wind conditions with wind speeds of 2 m/s ~ 10 m/s and wind angles of 60° ~ 120°, as shown in Table 1.

Table 1. Table of Environmental Wind Simulation Conditions

Serial Number	Wind speed	Wind direction angle	Tunnel length
A1 ~ A5	2 m/s		
A6 ~ A10	4 m/s		
A11 ~ A15	6 m/s	60°、75°、90°、105°、120°	110 m
A16 ~ A20	8 m/s		
A21 ~ A25	10 m/s		
A26 ~ A27	4 m/s	90°	150 m、200 m

Based on the above simulations, the characteristics of flow field distribution in one end blocking tunnel under different tunnel lengths were studied by taking the ambient wind conditions of 4m/s wind speed and 90° wind angle.

3 Results and discussion

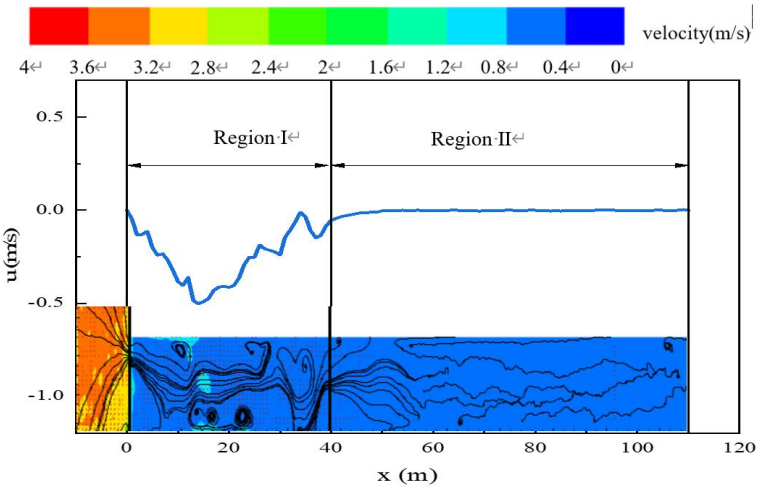

Fig. 2. Flow field distribution in tunnel under the influence of ambient wind

Fig. 2 presents the flow field distribution at y=0 m in one end of the blocked tunnel under the influence of an ambient wind speed of 4 m/s and an ambient wind angle α of 90°. The upper part of Fig. 2 illustrates the longitudinal velocity distribution of measurement points at z=2.5 m along the center axis of the tunnel, while the lower part

exhibits the cross-sectional flow field distribution at y=0 m. Evidently, Fig. 2 reveals that the flow field inside the tunnel can be categorized into two distinct regions: Region I corresponds to the vortex region, significantly influenced and disturbed by the ambient wind; meanwhile, Region II represents the stable region, displaying minimal impact from the ambient wind.

Upon a comprehensive analysis of the upper and lower sections of Fig. 2, it is evident that the velocity measurements taken at the boundary between the stabilized and vortex zones approximate 0.05 m/s. Consequently, the extent of the vortex region induced by the perturbing ambient wind, denoted as L_{eddy}, is characterized as the segment within the tunnel's span where the velocity recorded at the measurement point surpasses 0.05 m/s.

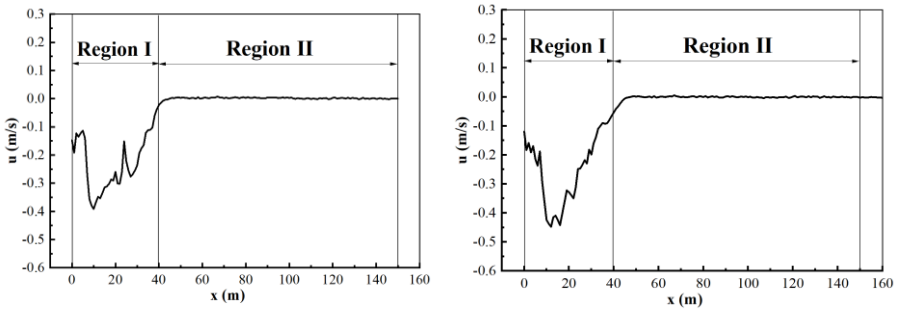

(a)Tunnel length 150m (b)Tunnel length 200m

Fig. 3. Flow field distribution in tunnel under the influence of ambient wind

Fig. 3 portrays the flow field distribution within the tunnel's one end under the conditions of varying tunnel lengths (150 m and 200 m), while subject to an ambient wind speed of v = 4 m/s and an ambient wind angle α = 90°. Figure 4 offers insights indicating that alterations in tunnel length exert negligible influence on the length of the vortex region, L_{eddy}.

Presented in Fig. 4 are velocity measurements taken subsequent to the stabilization of the flow field at the measurement point situated at z=2.5 m along the central axis of the blocked tunnel's one end.

These measurements were conducted under diverse wind speeds and wind directions. Notably, the velocity value within the stabilized region approximates 0.05 m/s.

Through meticulous data organization, the vortex region's length, L_{eddy}, was determined under various wind speeds and directions. The size of the vortex region length L_{eddy} is positively correlated with the wind speed v and negatively correlated with the wind angle α. In order to quantitatively analyze the effect of ambient wind on the flow field inside one end of the blocked tunnel, the ratio of L_{eddy} to the length of the tunnel is defined as the dimensionless vortex region length of the ambient wind on one end of the blocked tunnel, i.e.:

$$L^*_{eddy} = L_{eddy}/L_{tunnel} \tag{1}$$

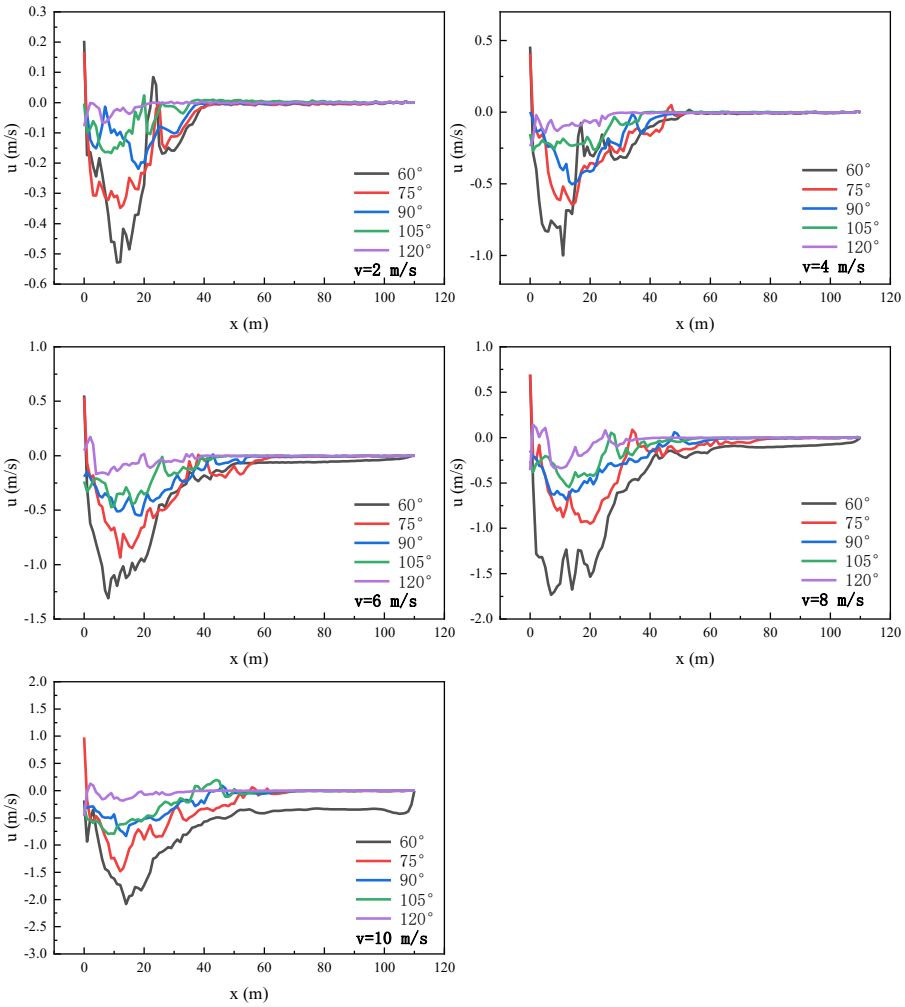

Fig. 4. Data of velocity measuring points in tunnel under different wind speed and direction

Table 2 elucidates that over the range of ambient wind speeds spanning from 2 m/s to 8 m/s, the dimensionless vortex region length, denoted as L^*_{eddy}, exhibits a nearly linear augmentation alongside the escalation of wind speed. However, at an ambient wind speed of 10 m/s, the dimensionless vortex region length, L^*_{eddy} demonstrates only minor variance when juxtaposed with the value at 8 m/s. This occurrence could be attributed to the tunnel's obstructive presence, leading to a subdued impact of altered ambient wind speeds on the perturbation of the flow field within the tunnel. Consequently, beyond a certain threshold wind speed, any subsequent increase appears to exert minimal influence on the dimensions of the dimensionless vortex region L^*_{eddy}.

Table 2. L^*_{eddy} in different wind velocity and direction

	60°	75°	90°	105°	120°
2 m/s	0.336364	0.318182	0.3	0.218182	0.063636
4 m/s	0.409091	0.418182	0.363636364	0.327273	0.209091
6 m/s	0.8	0.509091	0.481818182	0.345455	0.3
8 m/s	0.972727	0.663636	0.509090909	0.381818	0.309091
10 m/s	0.990909	0.590909	0.545454545	0.490909	0.245455

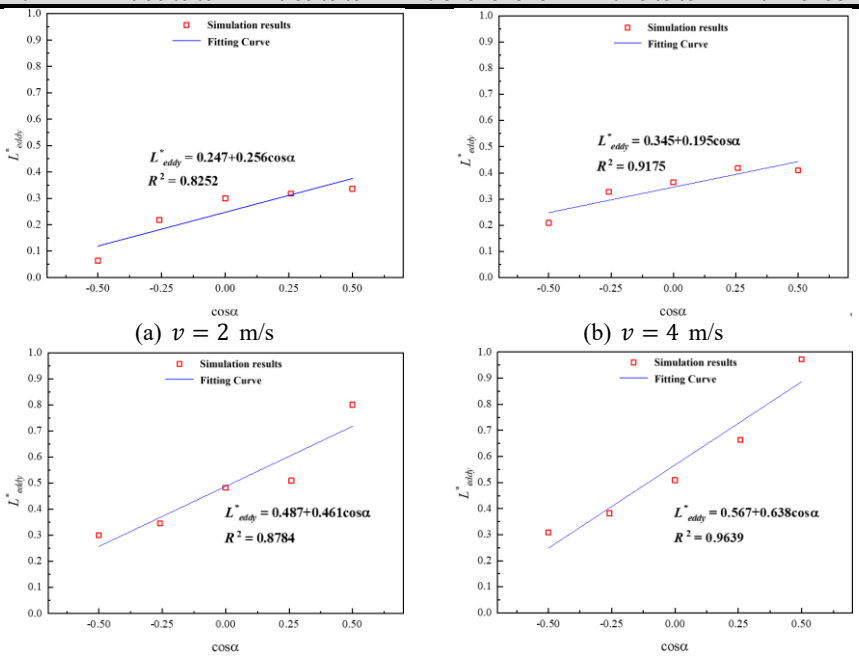

(a) $v = 2$ m/s (b) $v = 4$ m/s

(c) $v = 6$ m/s (d) $v = 8$ m/s

Fig. 5. L^*_{eddy} under different ambient wind direction

The data presented in Table 2 elucidates a discernible negative correlation between L^*_{eddy} and the magnitude of the wind angle α. The wind speed component aligned with the tunnel's axial direction notably influences the internal flow dynamics. The axial component of the ambient wind speed along the tunnel is denoted as follows:

$$v_x = v \cos \alpha \tag{2}$$

For α ∈ [60°, 120°], the axial wind speed v_x decreases as α increases, gradually transitioning from positive to negative values. Subsequently, a regression and analysis of L^*_{eddy} and cosα are performed for ambient wind speeds ranging from 2 m/s to 8 m/s.

The obtained fitting outcomes are graphically depicted in Fig. 5. Evidently, Fig. 5 demonstrates a robust linear correspondence between L^*_{eddy} and cosα, when wind speed remains constant.

The cumulative findings from the aforementioned analysis emphasize the robust linear interrelation of L^*_{eddy} with both v and cosα within the ranges v∈[2 m/s, 8 m/s] and a∈[60°, 120°]. A binary linear regression utilizing the dataset in Table 2 produces a predictive model for L^*_{eddy}.

$$L^*_{eddy} = 0.136 + 0.388\,cos\,\alpha + 0.055v \quad (3)$$

$$R^2 = 0.8376,\ v \in [2\,m/s,\ 8\,m/s],\ \alpha \in [60°,\ 120°]$$

Comparisons between the L^*_{eddy} prediction model and the simulation outcomes are showcased in Figure 6. Remarkably, Figure 6 underscores the superior predictive capacity of Eq. (3) for L^*_{eddy}.

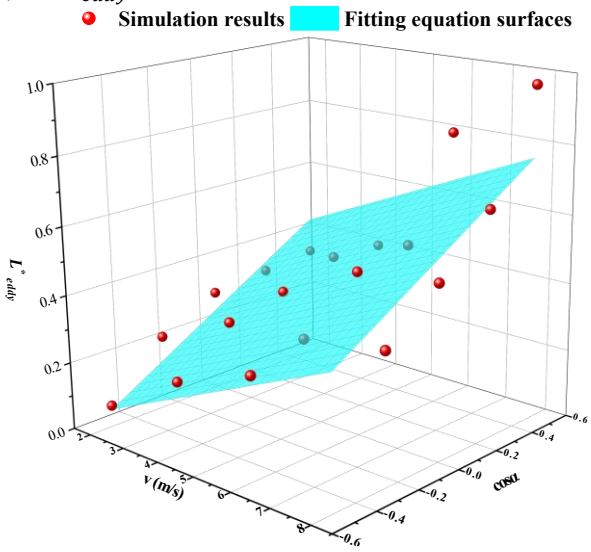

Fig. 6. Forecasting model of L^*_{eddy}

4 Conclusion

The external ambient wind introduces disturbances to the flow field within the blocked tunnel's one end, thereby delineating two discernible regions: the vortex region, which exhibits heightened susceptibility to ambient wind perturbations, and the wind-undisturbed region, which remains relatively unaffected by the ambient wind. Across ambient wind speeds ranging from 2 m/s to 8 m/s and wind angles spanning 60° to 120°, the extent of the vortex zone, L_{eddy}, manifests a positive correlation with wind speed, *v*, while manifesting a negative correlation with wind angle, α. Nevertheless, the influence of wind speed is observed to be modest. Remarkably, this influence dwindles in significance as ambient wind speeds surpass 8 m/s, whereby the enlargement of L_{eddy} no longer corresponds to the incremental escalation of wind speed.

This study delves into the analysis of flow fields within one end of obstructed tunnels, subject to the impacts of ambient wind. Such investigation serves to proffer valuable insights for applications in ventilation design, pollutant mitigation, and fire safety considerations.

Acknowledgments

This work was supported by the National Natural Science Foundation of China (Grant No. 52178064).

References

1. Nyman H, Sandberg M. The influence of external wind in tunnels [J]. International Journal of Ventilation, 10(1): 31-48(2011).
2. Kubwimana T, Salizzoni P, Bergamini E, et al. Wind-induced pressure at a tunnel portal [J]. Environmental Fluid Mechanics , 18(3): 769-86(2018).
3. Kubwimana T, Salizzoni P, Bergamini E, et al. Wind-induced pressure at a tunnel portal [J]. Environmental Fluid Mechanics, 18(3): 769-86 (2018).
4. Yu H, Jiang W, et al. Simulation study on random walk diffusion in the wake zone of exhaust emission towers [J]. Journal of Aerodynamics, (03): 349-54 (1996)
5. Yang Y, He C, et al. Field Measurement and Study on the Concentration Diffusion of Exhaust Gas at the Exit of Extra Long Highway Tunnel [J]. Journal of Underground Space and Engineering, (02): 392-6 (2008)
6. Yang Y, He C, et al. Numerical simulation of the impact of exhaust gas pollution at the entrance of a double hole highway tunnel [J]. Modern Tunnel Technology, (02): 94-8 (2009)
7. Peng K. Study on optimization of ventilation scheme of super long highway adjacent to Ventilation shaft based on the influence of pollutant channeling [D]. Southwest Jiaotong University (2019).
8. Chen T, Li Y, Luan D, et al. Study of flow characteristics in tunnels induced by canyon wind [J]. Journal of Wind Engineering and Industrial Aerodynamics, 202: 104236(2020).
9. Jing H, Liao H, Ma C, et al. Field measurement study of wind characteristics at different measuring positions in a mountainous valley [J]. Experimental Thermal and Fluid Science, 112: 109991(2020).
10. Minehiro, T, Fujita, K, Kawabata, N, Tanaka, F. Backlayering distance of thermal fumes in tunnel fire experiments using a large-scale model [J]. Fluid Sci. Technol. 7, 389–404(2012).
11. Santiago, J.L., Martilli, A, Martín, F. CFD simulation of airflow over a regular array of cubes. Part I: three-dimensional simulation of the flow and validation with wind-tunnel measurements. Bound.-Layer Meteorol. 122, 609–634(2006).
12. Zhou, Y., Yang, Y., Jiao, S.C., Zhang, L., Fan, C.G., Ding, C., Liu, X.P. Large Eddy Simulation of effectiveness of solid screen on improving natural ventilation performance in urban tunnels[J]. Tunnelling Underground Space Technol. 86, 174–185(2019).
13. Weng, M., Obadi, I., Wang, F., Liu, F., & Liao, C. Optimal distance between jet fans used to extinguish metropolitan tunnel fires: A case study using fire dynamic simulator modeling[J]. Tunnelling and Underground Space Technology, 95, 103116 (2020).
14. Chow W K. Dispersion of carbon monoxide from a vehicular tunnel with the exit located along a hillside [J]. Tunnelling and Underground Space Technology, 4(2): 231-4(1989).